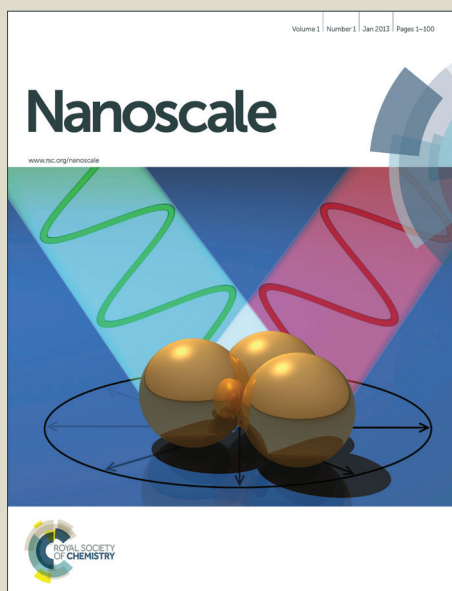


Nanoscale

Accepted Manuscript



This is an *Accepted Manuscript*, which has been through the Royal Society of Chemistry peer review process and has been accepted for publication.

Accepted Manuscripts are published online shortly after acceptance, before technical editing, formatting and proof reading. Using this free service, authors can make their results available to the community, in citable form, before we publish the edited article. We will replace this *Accepted Manuscript* with the edited and formatted *Advance Article* as soon as it is available.

You can find more information about *Accepted Manuscripts* in the [Information for Authors](#).

Please note that technical editing may introduce minor changes to the text and/or graphics, which may alter content. The journal's standard [Terms & Conditions](#) and the [Ethical guidelines](#) still apply. In no event shall the Royal Society of Chemistry be held responsible for any errors or omissions in this *Accepted Manuscript* or any consequences arising from the use of any information it contains.

COMMUNICATION

Monodisperse SnSb Nanocrystals for Li-ion and Na-ion Battery Anodes: Synergy and Dissonance Between Sn and Sb

Cite this: DOI: 10.1039/x0xx00000x

Received 00th January 2012,

Accepted 00th January 2012

DOI: 10.1039/x0xx00000x

www.rsc.org/

Meng He,^{a,b,§} Marc Walter,^{a,b,§} Kostiantyn V. Kravchyk,^{a,b,§} Rolf Erni,^c Roland Widmer,^d and Maksym V. Kovalenko^{a,b,*}

ABSTRACT. We report a facile chemical synthesis of monodisperse colloidal SnSb nanocrystals (NCs) via reaction between Sn NCs and SbCl₃ in oleylamine under reducing conditions. In comparison with individual Sn and Sb NCs and their mixtures, we show that through the creation of SnSb alloyed NCs the Li-ion storage properties are enhanced due to combination of high cycling stability of Sb with higher specific Li-ion storage capacity of Sn. In particular, stable capacities of above 700 and 600 mAh g⁻¹ were obtained after 100 cycles of charging/discharging at 0.5C and 4C-rates, respectively (1C corresponding to a current density of 660 mA g⁻¹). Furthermore, Na-ion storage capacities of >350 mAh g⁻¹ and >200 mAh g⁻¹ were obtained at 1C and 20C-rates, respectively. This study highlights the differences between Li- and Na-ion (electro)chemistries and great utility of monodisperse NCs as model systems for understanding size- and compositional effects on the performance of conversion-type electrode materials.

Monodisperse inorganic nanocrystals (NCs) and nanoparticles (NPs) can serve as well-defined model systems for controlling and studying the effects of the primary particle size, composition and morphology of electrode materials on their reversible electrochemical cycling in Li-ion batteries (LIBs) and in emerging, analogous Na-ion battery technology (SIBs). Particularly interesting are NCs and NPs of anode materials which operate via alloying with either Li (Si, Sn, Sb, Ge) or Na (Sn, Sb, P).¹⁻⁴ These alloys (*e.g.* Li₃Sb, Na₃Sb, Li₂₂Si₅ etc.) provide theoretical charge storage capacities 2-10 higher than that of commercially used graphite anodes (372 mAh g⁻¹ for LiC₆). Notably, graphite stores negligible amounts of Na-ions, indicating an urgent need for research towards stable Na-ion anode materials. All aforementioned alloying materials undergo massive volume changes by 100-400% upon full lithiation or sodiation, leading to mechanical destruction of the electrodes. Downsizing of the active material primary size to nanoscopic forms is presently studied as a major approach for mitigating the effects of the volume changes and to enhance the reaction kinetics.⁵⁻⁸ In this regard, we recently demonstrated clear size-dependence of both cycling stability and rate capability by using precisely engineered, 10-20nm large NCs of Sn⁹ and Sb¹⁰ as Li- and Na-ion storage media.

The question which had triggered this study - can one further tailor the electrochemical properties by combining two or more active materials in a well-controlled fashion, that is using pre-engineered monodisperse NCs? Will this combined effect be an

enhancement over individual properties of nanoscopic Sn and Sb, an average of two, or deterioration? Furthermore, Li-ion and Na-ion electrochemistries of the same electrode material are often considerably different.^{11,12} We therefore thought to study Li-ion and Na-ion storage properties of monodisperse SnSb NCs and compare the results with individual Sn and Sb NCs and their mixtures. Although there have been several previous studies on SnSb electrodes for LIBs and SIBs,¹³⁻²² the questions raised here require obtaining Sn, Sb and SnSb in the form of uniform colloidal NCs of very similar size. In the following, we present a facile colloidal synthesis of monodisperse SnSb NCs. Then we show that Li-ion storage properties of SnSb NCs are significantly enhanced as compared to individual Sn, Sb NCs and their mixtures, both in terms of charge storage capacity and cycling stability. As a result, high charge storage capacities above 700 and 600 mAh g⁻¹ were obtained after 100 cycles of charging/discharging at 0.5C and 4C-rates, respectively (1C corresponding to a current density of 660 mA g⁻¹). In Na-ion cells, on contrary, we find that the presence of Sn reduces the overall Na-ion storage capacity to ca. 350 mAh g⁻¹ and 200 mAh g⁻¹ at 1C and 20C-rates, respectively, while maintaining high cycling stability and high rate capability.

SnSb NCs were obtained *via* a successive reduction of the respective Sn and Sb precursor in a one-pot synthesis (Figure 1, for details, see Electronic Supplementary Information). First, Sn NC seeds were synthesized according to our previously reported procedure.⁹ Ten seconds after the nucleation of Sn NCs, the Sb precursor was injected into the hot solution at 210 °C. Within several minutes the Sn-Sb alloy was formed, as can be illustrated by XRD patterns (Figure 2), and after ripening for several hours uniform ~20nm SnSb NCs with narrow size distribution (<10%, Figures S1 and S2 of SI) were obtained. In this reaction, inexpensive tin (II) and antimony (III) chlorides are used as precursors, while lithium bistrimethylsilylamide [LiN(SiMe₃)₂] serves as a mild base for partial deprotonation of oleylamine according to the acid-base equilibrium: R-NH₂ + LiN(SiMe₃)₂ ↔ R-NHLi + HN(SiMe₃)₂. The Sn/Sb-oleylamide species are then formed *in-situ* via the reaction of Li-oleylamide with Sn (II)/Sb (III) chlorides,^{9,10} and serve as the actual precursors being reduced (Sn) or thermally decomposed (Sb). It should be pointed out that the simultaneous injection of Sn and Sb chlorides leads only to the formation of Sb NCs (Figure S3A of SI)

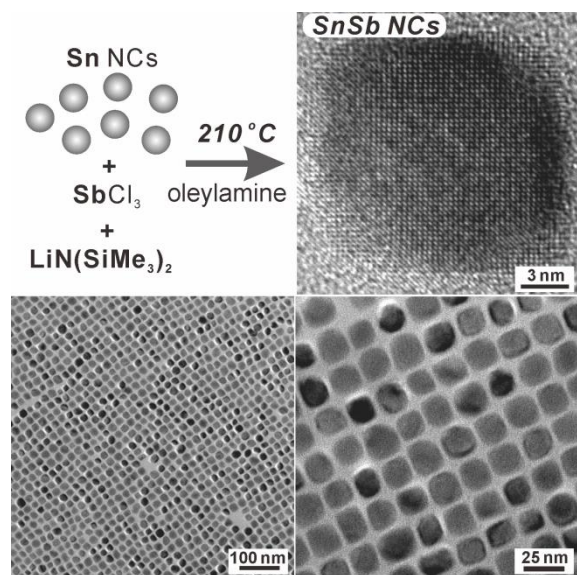


Figure 1. (A) Schematics of one-pot synthesis of SnSb NCs, along with high- and low-resolution transmission electron microscopy (TEM) images of ~ 20 nm SnSb NCs.

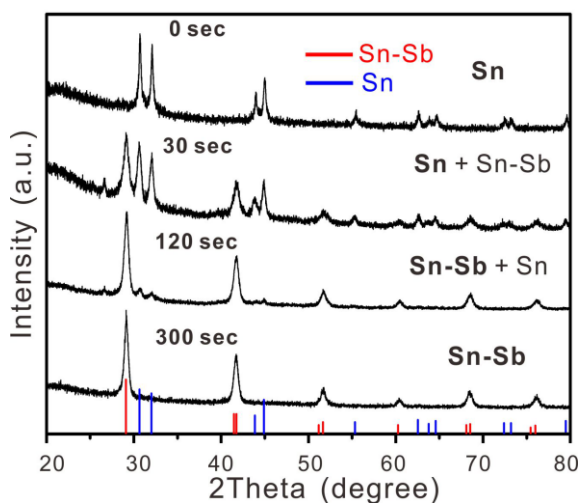


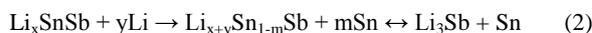
Figure 2. Evolution of powder X-ray diffraction (XRD) patterns during the conversion of Sn NCs into SnSb NCs.

due to the higher reactivity (instability) of the Sb precursor. Equally important is not to age Sn seeds for too long before adding the Sb precursor, as this may lead to the mixture of Sn and SnSb phases (Figure S3B). High-resolution TEM images (Figure 1) demonstrate the crystallinity of SnSb NCs. Elemental mapping with energy dispersive X-ray spectroscopy in scanning TEM mode (EDX-STEM) suggest uniform alloying (Figure S4). Rietveld refinement of XRD patterns (Figure S5) matches the known rhombohedral crystal structure of β -SnSb.²³ β -SnSb has essentially a cubic NaCl-type structure with a slight rhombohedral distortion ($a_{\text{rtho}} \sim 6.13$ Å, $\alpha \sim 89.6^\circ$). This can explain the propensity to form cubic or truncated cubic NCs. The Sn:Sb atomic ratio was 3:2, as estimated by EDX analysis and verified by inductively coupled plasma-optical emission spectrometry (ICP-OES; Table S1). This composition agrees well with the reported homogeneity region of ± 10 at% in β -SnSb.^{23, 24}

Before testing the performance of SnSb NCs as anode material in LIBs and SIBs, the insulating long-chained capping ligands were removed by treating with 1M solution of hydrazine in acetonitrile, a method commonly used for improving charge transport in quantum dot solids²⁵⁻²⁷ and previously used for Sn, Sb and SnGe NC anodes.^{9, 10, 28} All electrodes were tested under the same conditions in coin-type half-cells with metallic Li or Na as counter electrodes. Working electrodes contained 64wt% of active material, carboxymethylcellulose (CMC, 15 wt%) as a polymer binder, and amorphous carbon as conductive additive (21%). The films were casted from aqueous slurries and after vacuum drying had similar mass loading of ~ 0.5 mg/cm². Fluoroethylenecarbonate (FEC) was used as electrolyte additive for stabilizing the solid-electrolyte interface (SEI).⁸

SnSb NCs as LIB anodes. So far, very few reports have dealt with micro- and nanoscopic SnSb powders as anode materials in LIBs.^{13-19, 22} The best performances were characterized by the capacities of up to 500-600 mAh g⁻¹ (0.2C-rate), obtained for mechanochemically synthesized nanocomposites of SnSb with carbon.^{19, 22}

Figure 3A compares the capacities and cycling stabilities obtained for SnSb NCs and, for comparison, for individual Sn and Sb NCs and their mixture. Owing to the SEI formation and reduction of surface oxides (see Figure S11 for XPS spectra), coulombic efficiencies of 40-50% were obtained for the first cycle, but approached 97-99% during subsequent cycling. In accordance with the higher theoretical capacity of Sn (992 mAh g⁻¹) vs. Sb (660 mAh g⁻¹), all Sn-containing electrodes showed higher initial capacities than pure Sb NCs. At the same time, pure Sn NCs showed lowest cycling stability. Alloying with Sb allowed combining excellent cycling stability and rate capability of Sb (see Figure 3 and Ref.¹⁰) with higher capacity of Sn. High cycling stability and rate capability of Sb have been previously ascribed^{10, 29} to smaller volumetric expansion upon full lithiation ($\Delta V = 135\%$), fewer number of intermediate crystalline phases during cycling (only one – Li₂Sb), as compared to Sn ($\Delta V = 300\%$, 7 crystalline Li-Sn alloys),³ and faster Li-ion diffusion in the layered structure of Sb. Importantly, at higher current density of 2.64A g⁻¹ (4C-rate) alloyed SnSb NCs possess much higher cycling stability than the mechanic mixtures of Sn and Sb NCs of the same size (Figure 3B). Capacities of at least 700 and 600 mAh g⁻¹ can be obtained after 100 cycles of charging/discharging at 0.5C and 4C-rates. Important hints into the origin of this difference are provided by differential capacity plots (dQ/dV), shown for the 10th and 80th cycles (Figures 4A, S6), and by cyclic voltammograms (CVs, Figure S6). For both SnSb nanoalloys and Sb/Sn NC mixtures, dQ/dV plots and CVs are the sum of the curves obtained for Sn and Sb NCs. This is in agreement with previous in-situ XRD studies showing that lithiation of SnSb produces crystalline Li₃Sb and amorphous Li_zSn alloys:^{21, 30, 31}



However, compared to the bulk material dQ/dV peaks for SnSb nanoalloys the are much broader. Such broadening is often attributed to very small crystallite size during the cycling, since at the nanoscale the electrochemical reactions are known to occur within much broader voltage intervals. Accordingly, the superior cycling stability of SnSb nanoalloys can be explained by much smaller mean crystallite size during the electrochemical cycling.

SnSb NCs as Na-ion anode materials. The search for efficient anode materials for SIBs is critically important because well-studied Li-ion anode materials such as graphite or silicon uptake negligible

amounts of Na-ions.^{32,33} In the first cycles, Na-ion charge storage capacities of SnSb NCs were 360-370 mAh g⁻¹ at 0.5C-rate (Figure

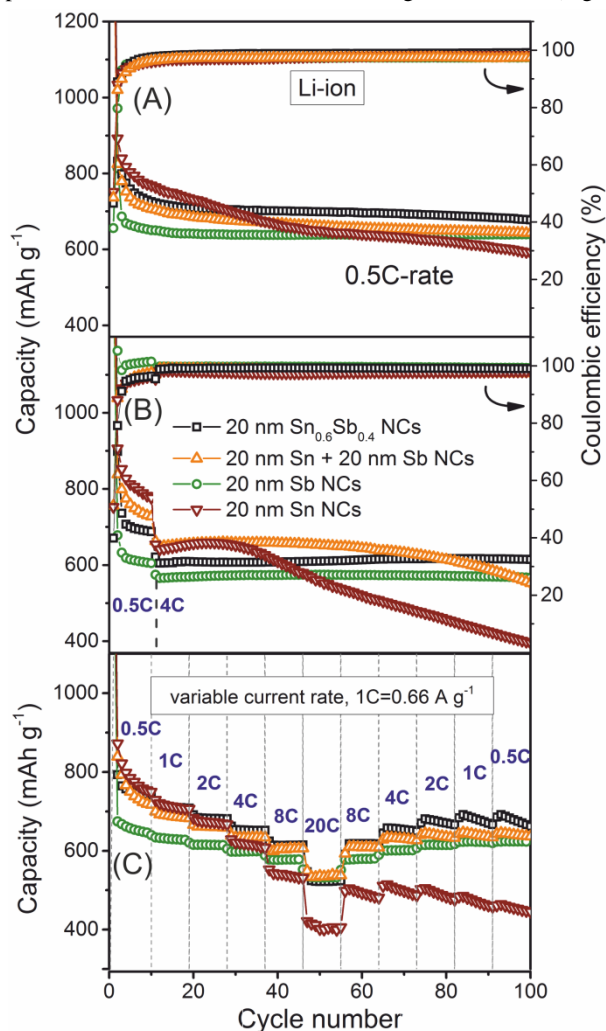


Figure 3. (A, B) Galvanostatic cycling stability tests at current densities of 0.33 A g⁻¹ and 2.64 A g⁻¹, and (C) rate capability tests (0.5-20C rates, 1C=660 mA g⁻¹ based on the theoretical capacity of pure Sb) for Li-ion anodes composed of SnSb, Sn and Sb NCs. First two cycles for all electrodes shown in (B, C) were carried out at 0.1C rate. All batteries were cycled in the voltage window of 0.02-1.5 V.

5A). Upon subsequent cycling at 1C and 20C rates, stable capacities of 350 mAh g⁻¹ and 230 mAh g⁻¹ respectively, were maintained for more than 100 cycles. Rate-capability tests at 0.5-20C rate showed full capacity recovery, or even higher capacities after the moderate cycling rate of 0.5C is resumed (Figure 5B). To our knowledge, this is the first study showing high rate-capability and stability at high current rates in SnSb anodes. Coulombic efficiencies were 97-98% (higher for 0.5C-rates), still indicating suboptimal stability of the SEI layer.

Should there be full sodiation to Na₃Sb (660 mAh g⁻¹) and Na₁₅Sn₄ (847 mAh g⁻¹), the capacity of SnSb NCs must reach 750 mAh g⁻¹. Instead, our results and three recent reports^{20, 21, 34} show similar capacities of 300-400 mAh g⁻¹ at 0.2-1C rates. This is where the difference between Li and Na-ion insertion chemistries may come into play. While the performance of SnSb electrodes in LIBs can be considered as addition of Sn and Sb vs. Li., plus the

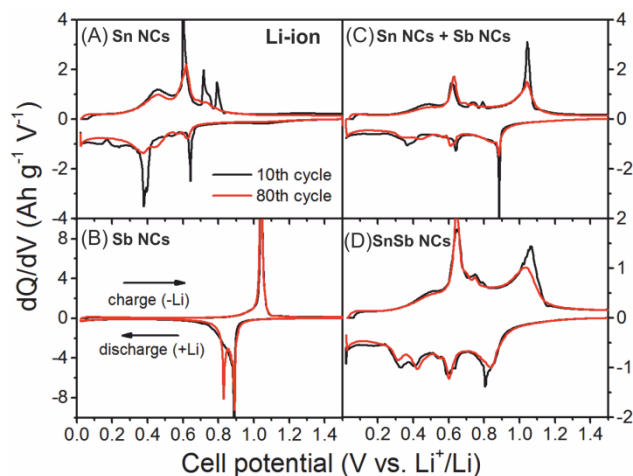


Figure 4. Differential capacity plots obtained from galvanostatic discharge/charge curves during 10th and 80th cycles at a current density of 0.33 A g⁻¹

stabilizing effect of nanosizing and of atomic intermixing, the alloying chemistry of SnSb-based SIB anodes is clearly different from pure Sn and Sb. This can be clearly seen from dQ/dV plots and in CVs (Figures 5A and S7). Recent in-situ XRD studies of Darwiche *et al.*²¹ have shown that sodiation and desodiation of SnSb leads to products without resolvable XRD peaks, consistent with very broad electrochemical features. We also hypothesize that in SnSb composite the sodiation of Sn is incomplete, as it extends below 0.02V vs. Li. dQ/dV plots and CV of Sn NC electrodes showed that more than 50% of Na-ions are inserted at very low potentials and sodiation is at steepest rise at 0.02V (Figure S7), with stable capacities of 350 mAh g⁻¹ maintained for 100 cycles at 0.2C-rate (Figure S8). Large volume change ($\Delta V=420\%$ for Sn \rightarrow Na₁₅Sn₄ transition), lower voltage of alloying and slower diffusion of Na-ion leads to incomplete sodiation and far poorer cycling of Sn vs. Na than vs. Li.^{35, 36}

In summary, we report a facile colloidal synthesis of alloyed SnSb NCs. In comparison with individual Sn and Sb NCs, we show that through the creation of SnSb alloyed NCs the Li-ion storage properties are enhanced due to combination of high cycling stability of Sb with higher specific Li-ion storage capacity of Sn. In particular, stable capacities of above 700 and 600 mAh g⁻¹ were obtained after 100 cycles of charging/discharging at 0.5C and 4C-rates. Furthermore, Na-ion storage capacities of >350 mAh g⁻¹ and >200 mAh g⁻¹ were obtained at 1C and 20C-rates, respectively. In Na-ion anodes, mainly Na_xSb phase is formed, whereas Sn contributes only a marginal capacity. This study points to the important differences between Na- and Li-ion chemistries and to the advantages provided by monodisperse NCs for understanding of electrochemical properties of nanoscopic electrode materials.

Acknowledgements

M. He, M. Walter and K. Kravchik contributed equally to this work. We acknowledge financial support from the Swiss National Science Foundation (SNF-Project Nr. 200021_140245), Swiss Federal Commission for Technology and Innovation (CTI-Project Nr. 14698.2 PFIW-IW) and CTI Swiss Competence Centers for Energy Research (SCCER Heat and Electricity Storage). We thank Dr. Maksym Yarema for fruitful discussions. Electron microscopy was performed at Empa Electron Microscopy Center.

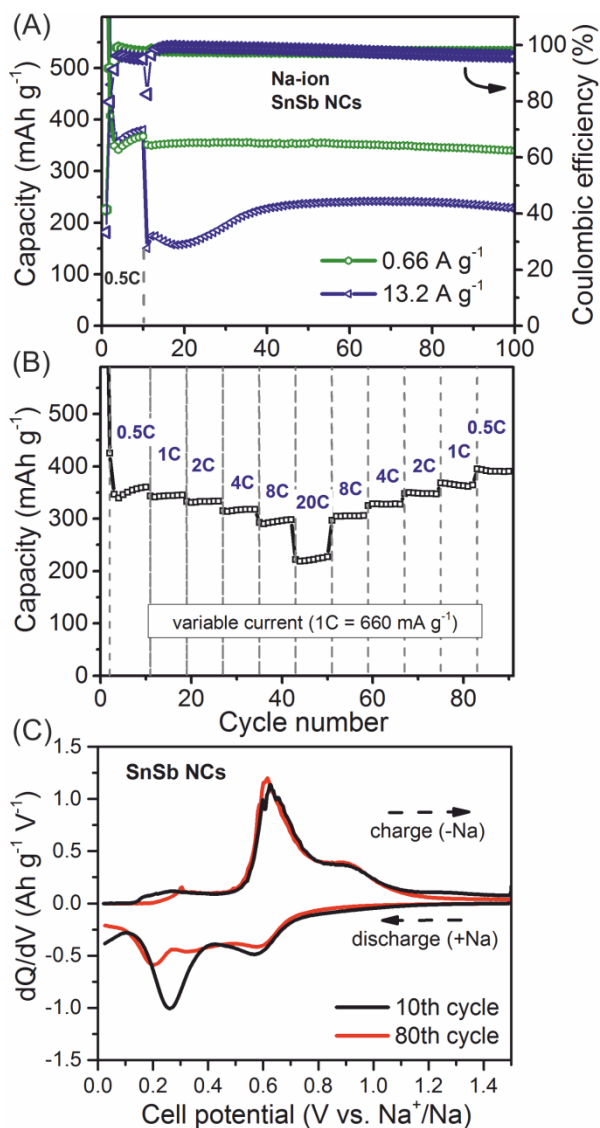


Figure 5. (A) Galvanostatic cycling stability tests at 1C and 20C rates, and (B) rate capability tests (0.5-20C rates, 1C=660 mA g⁻¹) for Na-ion anodes comprising SnSb NCs as storage material. First two cycles for all electrodes shown in (A, B) were carried out at 0.1C rate. (C) Differential capacitance plots corresponding to 10th and 80th cycles at 1C-rate. All batteries were cycled at voltages of 0.02-1.5 V.

Notes and references

^aETH Zürich – Swiss Federal Institute of Technology Zürich, Vladimir Prelog Weg 1, CH-8093, Zürich, Switzerland

^bEmpa-Swiss Federal Laboratories for Materials Science and Technology, Laboratory for thin films and photovoltaics, CH-8600 Dübendorf, Switzerland

^cElectron Microscopy Center, Empa – Swiss Federal Laboratories for Materials Science and Technology, CH-8600 Dübendorf, Switzerland

^dNanotech@surfaces Laboratory, Empa – Swiss Federal Laboratories for Materials Science and Technology, CH-8600 Dübendorf, Switzerland

^ethese authors contributed equally

†Electronic Supplementary Information (ESI) available: materials and methods, additional structural and electrochemical characterization. See DOI: 10.1039/c000000x/

- C. M. Hayner, X. Zhao and H. H. Kung, *Annu. Rev. Chem. Biomol. Eng.*, 2012, **3**, 445-471.
- V. Palomares, M. Casas-Cabanas, E. Castillo-Martínez, M. H. Han and T. Rojo, *Energ. Environ. Sci.*, 2013, **6**, 2312-2337.
- C.-M. Park, J.-H. Kim, H. Kim and H.-J. Sohn, *Chem. Soc. Rev.*, 2010, **39**, 3115-3141.
- Y. Kim, Y. Park, A. Choi, N. S. Choi, J. Kim, J. Lee, J. H. Ryu, S. M. Oh and K. T. Lee, *Adv. Mater.*, 2013, **25**, 3045-3049.
- C. K. Chan, H. Peng, G. Liu, K. McIlwrath, X. F. Zhang, R. A. Huggins and Y. Cui, *Nat. Nanotech.*, 2008, **3**, 31-35.
- A. Magasinski, P. Dixon, B. Hertzberg, A. Kvit, J. Ayala and G. Yushin, *Nat. Mater.*, 2010, **9**, 353-358.
- I. Kovalenko, B. Zdyrko, A. Magasinski, B. Hertzberg, Z. Milicev, R. Burtovyy, I. Luzinov and G. Yushin, *Science*, 2011, **334**, 75-79.
- A. M. Chockla, K. C. Klavetter, C. B. Mullins and B. A. Korgel, *Chem. Mater.*, 2012, **24**, 3738-3745.
- K. Kravchuk, L. Protesescu, M. I. Bodnarchuk, F. Krumeich, M. Yarema, M. Walter, C. Guntlin and M. V. Kovalenko, *J. Am. Chem. Soc.*, 2013, **135**, 4199-4202.
- M. He, K. Kravchuk, M. Walter and M. V. Kovalenko, *Nano Lett.*, 2014, 1255-1262.
- S.-W. Kim, D.-H. Seo, X. Ma, G. Ceder and K. Kang, *Adv. Energy Mater.*, 2012, **2**, 710-721.
- S. Y. Hong, Y. Kim, Y. Park, A. Choi, N.-S. Choi and K. T. Lee, *Energ. Environ. Sci.*, 2013, **6**, 2067-2081.
- L. Shi, H. Li, Z. Wang, X. Huang and L. Chen, *J. Mater. Chem.*, 2001, **11**, 1502-1505.
- S. A. Needham, G. X. Wang and H. K. Liu, *J. All. Comp.*, 2005, **400**, 234-238.
- G. Zhang, K. Huang, S. Liu, W. Zhang and B. Gong, *J. All. Comp.*, 2006, **426**, 432-437.
- H. Zhao, C. Yin, H. Guo and W. Qiu, *Electrochem. Solid. St.*, 2006, **9**, A281.
- C. M. Park and K. J. Jeon, *Chem. Commun.*, 2011, **47**, 2122-2124.
- J. Li, Q. Ru, S. Hu, D. Sun, B. Zhang and X. Hou, *Electrochim. Acta*, 2013, **113**, 505-513.
- J.-U. Seo and C.-M. Park, *J. Mater. Chem. A.*, 2013, **1**, 15316.
- L. Xiao, Y. Cao, J. Xiao, W. Wang, L. Kovarik, Z. Nie and J. Liu, *Chem. Commun.*, 2012, **48**, 3321-3323.
- A. Darwiche, M. T. Sougrati, B. Fraisse, L. Stievano and L. Monconduit, *Electrochem. Commun.*, 2013, **32**, 18-21.
- C.-M. Park and H.-J. Sohn, *Electrochim. Acta*, 2009, **54**, 6367-6373.
- L. Norén, R. L. Withers, S. Schmid, F. J. Brink and V. Ting, *J. Sol. Stat. Chem.*, 2006, **179**, 404-412.
- V. Vassiliev, M. Lelaurain and J. Hertz, *J. All. Comp.*, 1997, **247**, 223-233.
- M. Law, J. M. Luther, Q. Song, B. K. Hughes, C. L. Perkins and A. J. Nozik, *J. Am. Chem. Soc.*, 2008, **130**, 5974-5985.
- D. V. Talapin and C. B. Murray, *Science*, 2005, **310**, 86-89.
- H. Zhang, B. Hu, L. Sun, R. Hovden, F. W. Wise, D. A. Muller and R. D. Robinson, *Nano Lett.*, 2011, **11**, 5356-5361.
- M. I. Bodnarchuk, K. V. Kravchuk, F. Krumeich, S. Wang and M. V. Kovalenko, *ACS Nano*, 2014, **8**, 2360-2368.
- A. Darwiche, C. Marino, M. T. Sougrati, B. Fraisse, L. Stievano and L. Monconduit, *J. Am. Chem. Soc.*, 2012, **134**, 20805-20811.
- F. J. Fernández-Madriral, P. Lavela, C. P. Vicente, J. L. Tirado, J. C. Jumas and J. Olivier-Fourcade, *Chem. Mater.*, 2002, **14**, 2962-2968.
- L. Aldon, A. Garcia, J. Olivier-Fourcade, J.-C. Jumas, F. J. Fernández-Madriral, P. Lavela, C. P. Vicente and J. L. Tirado, *J. Power Sources*, 2003, **119-121**, 585-590.
- P. Ge and M. Foulletier, *Solid State Ionics*, 1988, **28-30, Part 2**, 1172-1175.
- S. Komaba, Y. Matsuura, T. Ishikawa, N. Yabuuchi, W. Murata and S. Kuze, *Electrochem. Commun.*, 2012, **21**, 65-68.

34. L. Ji, M. Gu, Y. Shao, X. Li, M. H. Engelhard, B. W. Arey, W. Wang, Z. Nie, J. Xiao, C. Wang, J.-G. Zhang and J. Liu, *Adv. Mater.*, 2014, DOI: 10.1002/adma.201304962.
35. Y. Xu, Y. Zhu, Y. Liu and C. Wang, *Adv. Energy Mater.*, 2013, **3**, 128-133.
36. Y.-M. Lin, P. R. Abel, A. Gupta, J. B. Goodenough, A. Heller and C. B. Mullins, *ACS Appl.Mater.Interfaces*, 2013, **5**, 8273-8277.

Table of Content Entry:

Precisely engineered SnSb nanocrystals provide a model experimental system for tuning and understanding Li-ion and Na-ion storage properties.

